Available online at www.sciencedirect.com
ScienceDirect
Journal of Sound and Vibration 299 (2007) 739–756
JOURNAL OF SOUND AND VIBRATION
www.elsevier.com/locate/jsvi

Stiffness matrices for flexural–torsional/lateral buckling and vibration analysis of thin-walled beam ☆

Nam-Il Kim[a], Chung C. Fu[b], Moon-Young Kim[c,*]

[a]*Department of Civil and Environmental Engineering, Myongji University, San 38-2, Nam-Dong, Yongin, Kyonggi-Do 449-728, Republic of Korea*
[b]*Department of Civil and Environmental Engineering, University of Maryland, College Park, MD 20742, USA*
[c]*Department of Civil and Environmental Engineering, Sungkyunkwan University, Cheoncheon-Dong, Jangan-Ku, Suwon 440-746, Republic of Korea*

Received 31 March 2005; received in revised form 3 May 2006; accepted 23 June 2006
Available online 2 October 2006

Abstract

Based on the power series method, the static and dynamic stiffness matrices for the flexural–torsional buckling and free vibration analysis of thin-walled beam with non-symmetric cross-section subjected to linearly variable axial force are newly presented. Additionally, the static stiffness matrix for the lateral buckling analysis of non-symmetric beam is presented for the first time. For this, the elastic strain energy, the potential energy considering the second-order terms of finite rotations, and the kinetic energy for thin-walled beam with non-symmetric cross-section are introduced. Then equations of motion and force–deformation relations are derived from the energy principle. Explicit expressions for displacement parameters are derived based on power series expansions of displacement components. Finally, the static and dynamic element stiffness matrices are determined using force–deformation relationships. In order to verify the accuracy of this study, the numerical solutions are presented and compared with the finite element solutions using the Hermitian beam elements and ABAQUS's shell elements.

1. Introduction

Thin-walled beams have been widely used as the most common load-carrying systems in many civil, mechanical and aerospace engineering applications, both in their stand-alone forms and as stiffeners for plate and shell structures. The thin-walled sections, such as I section, channel and angle, are appealing because they offer a high performance in terms of minimum weight for a given strength. However, it is well known that such weight-optimized members having arbitrary cross-sections are very susceptible to flexural–torsional and lateral buckling and display complex vibrational behavior. Therefore, the accurate prediction of their stability limit state and natural frequency is of fundamental importance in the design of thin-walled structures.

Up to the present, investigation into the stability and vibrational behavior of beam members has been carried out extensively since the early works of Vlasov [1] and Timoshenko and Gere [2]. Stability and

☆This is an original paper which has neither previously, nor simultaneously, in whole or in part, been submitted anywhere else.

*Corresponding author. Tel.: +82 31 290 7514; fax +82 31 290 7548.
E-mail address: kmye@skku.ac.kr (M.-Y. Kim).

0022-460X/$ - see front matter © 2006 Elsevier Ltd. All rights reserved.
doi:10.1016/j.jsv.2006.06.062

vibration analyses of beam become quite difficult problems when other than simple boundary conditions exist, where the cross-section has one or no axis of symmetry. Closed-form solutions are mathematically complex and exist only for a limited number of problems. Many numerical techniques such as finite element method have also been used to solve the stability of thin-walled beams. Barsoum and Gallagher [3], Chen and Atsuta [4] and Attard [5] presented a finite element formulation based on generalized displacement field. Kitipornchai and Trahair [6] modified Barsoum and Gallagher's formulation so that it could be applied to mono-symmetric beams. Robert and Burt [7] used the energy method to derive approximate formulas for simply supported mono-symmetric I-beams. Sun and Huang [8], in order to study impact problems, developed the mass and stiffness matrices for a beam element with fifth-order shape functions. Coulter and Miller [9] investigated the buckling and vibration of plane beam subjected to distributed axial force using the finite element method. Also, vibrational behavior of an initially stressed beam on discretely spaced elastic supports has been studied by Park et al. [10]. They derived a theoretical formulation of the system using the variational principle. Andrade and Camotim [11] presented a general variational formulation to analyze the lateral–torsional buckling behavior of singly symmetric thin-walled tapered beams. Their results were obtained by means of the Rayleigh–Ritz method, using trigonometric functions to approximate the beam critical buckling mode. The derivation and implementation of generalized beam theory was presented by Silvestre and Camotim [12], based fully analytical formulae to evaluate distortional bifurcation stresses in cold-formed steel C and Z-section column (uniform compression), beams (pure bending) and beam-columns (uniform compression + pure bending) with arbitrarily inclined single-lip stiffeners. Yu and Schafer [13] conducted a series of distortional buckling tests on cold-formed steel C and Z sections in bending to establish the capacity in distortional buckling failures. Also, a series of new flexural tests focused on the role of web slenderness in local buckling failures of C and Z sections was reported by Yu and Schafer [14].

Another effective approach solving the flexural–torsional buckling and vibration problems of beam is to develop the stiffness matrices based on the solution of the differential equation of beam. Most of those studies adopted an analytical method that required explicit expressions of exact displacement functions for governing equations (Friberg [15], Banerjee [16–18], Banerjee and Williams [19–21], Banerjee and Fisher [22], Leung and Zeng [23]). This procedure was very effective in saving the computing time due to the closed-form solution which can be easily derived by the help of symbolic computation. However, these analytical operations were often too complex to yield exact displacement functions in the case of solving a system of simultaneous ordinary differential equations with many variables. Also, those studies were restricted to the analysis of beam with doubly or mono-symmetric cross-sections. Lee et al. [24] presented a transfer matrix for three-dimensional vibration analysis of piping system containing fluid flow. For the lateral buckling analysis, Leung [25] presented the stiffness matrix of frame under a constant in-plane moment using the analytical method. Spillers and Rashidi [26] generated the member stiffness matrix of beam without warping effect under a concentrated load based on the series solution approach. However, they considered the beam with doubly symmetric section only.

Recently, Kim et al. [27] proposed the improved numerical method to exactly determine the static stiffness matrix for the flexural–torsional buckling analysis of thin-walled beam with non-symmetric section subjected to constant axial force and the dynamic stiffness matrix for free vibration analysis. In their study, they transformed a set of the second-order ordinary differential equations with constant coefficients into a set of the first order differential equations and solved the associated linear eigen-problem with non-symmetric matrices. However, unfortunately, their method is not valid any longer for the flexural–torsional buckling and free vibration analysis of thin-walled beam subjected to linearly variable axial force and the lateral buckling analysis of a beam subjected to a constant lateral force since the differential equations have the variable coefficients.

To resolve this shortcoming, this paper intends to present a new static and dynamic stiffness matrices for the flexural–torsional buckling and free vibration analysis of thin-walled beam with non-symmetric cross-section subjected to linearly variable axial force and the lateral buckling analysis based on the power series method. The important points presented are summarized as follows:

1. Equations of motion and force–displacement relations are derived from the total potential energy of a thin-walled beam with a non-symmetric cross-section subjected to linearly variable axial force and moment.
2. A numerical method to evaluate the static and dynamic element stiffness matrices of thin-walled beam is developed based on the power series expansions of displacement components.

3. In numerical examples, to demonstrate the accuracy and validity of this study, numerical solutions are presented and compared with finite element solutions using the Hermitian beam elements and ABAQUS's shell elements. Particularly, the influence of the constant and linearly variable axial force on the vibrational behavior of non-symmetric beam is investigated.

2. Equations of motion of thin-walled beam with non-symmetric cross-section

2.1. Total potential energy under consideration

For the stability analysis of space frame which consist of structural members with different directions in space, Argyris et al. [28,29] pointed out that most of the previous finite element formulation that include only the first-order terms of rotational parameters appear to be incorrect. It is largely due to deficiency of moment equilibrium conditions at the joint and the non-commutative nature of rotations about fixed axes. To resolve these difficulties, Argyris et al. introduced the semitangential rotations and semitangential moments that have mechanisms corresponding to Ziegler's [30] semitangential torque, and derived the geometric stiffness matrix of the space frame using the natural mode formulation. Chen and Blandford [31] formulated the large deformation theory of the thin-walled space frame by selecting Rodriguez vector components as the rotational displacement parameters. Teh and Clarke [32,33] indicated the awkwardness of a quasi-tangential and semitangential moment from the true behavior of internal moment and non-symmetry of the element tangent stiffness matrix, and they introduced the fourth kind of conservative moment and vectorial rotation.

In this study, the potential energy functional due to the initial axial force and bending moments is consistently used corresponding to semitangential moments because the potential energy due to the bending moments has been derived based on inclusion of second order terms of semitangential rotations.

For this, we consider seven displacement parameters and stress resultants defined at the coordinate system (x_1, x_2, x_3) are shown in Fig. 1. The x_1, axis coincides with the centroid; x_2, x_3, are not necessarily principal inertia axes; U_x, U_y, U_z and $\omega_1(=\theta)$, $\omega_2(=-U'_z)$, $\omega_3(=U'_y)$, are rigid body translations and rotations of the cross-section with respect to x_1, x_2 and x_3 axes, respectively, and $f(=-\theta')$ is the parameter defining warping of the cross-section.

The total displacement $\mathbf{U}$ can be written by the summation of the first- and second-order terms of the displacement parameters as

$$\mathbf{U}^{\mathrm{T}} = \left(U_1 + U_1^*, U_2 + U_2^*, U_3 + U_3^*\right), \tag{1}$$

where

$$U_1 = U_x - U'_z x_3 - U'_y x_2 - \theta' \phi, \tag{2a}$$

$$U_2 = U_y - \theta x_3, \tag{2b}$$

$$U_3 = U_z + \theta x_2 \tag{2c}$$

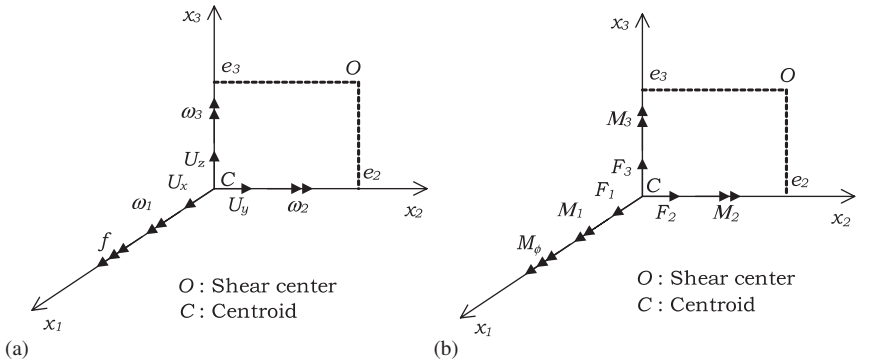

Fig. 1. Notation for displacement parameters and stress resultants: (a) displacement parameters, (b) stress resultants.

and

$$U_1^* = \frac{1}{2}\left[-\theta U'_z x_2 + \theta U'_y x_3\right], \tag{3a}$$

$$U_2^* = \frac{1}{2}\left[-\left(\theta^2 + U'^2_y\right)x_2 - U'_y U'_z x_3\right], \tag{3b}$$

$$U_3^* = \frac{1}{2}\left[-U'_y U'_z x_2 - \left(\theta^2 + U'^2_z\right)x_3\right]. \tag{3c}$$

In Eq. (1), U_i and U_i^* denote the first- and second-order terms of the displacement parameters, respectively. The 'prime' denotes derivative with respect to x_1. A complete set of linear and nonlinear strain–displacement relations for the thin-walled beam-columns are expressed as

$$e_{11} = U_{1,1} = U'_x - U''_z x_3 - U''_y x_2 - \theta''\phi, \tag{4a}$$

$$2e_{12} = U_{1,2} + U_{2,1} = -\theta'\phi_{,2} - \theta' x_3, \tag{4b}$$

$$2e_{13} = U_{1,3} + U_{3,1} = -\theta'\phi_{,3} + \theta' x_2, \tag{4c}$$

$$2\eta_{11} = U_{2,1}^2 + U_{3,1}^2 = \left(U'_y - \theta' x_3\right)^2 + \left(U'_z + \theta' x_2\right)^2, \tag{5a}$$

$$\begin{aligned} 2\eta_{12} &= U_{1,1}U_{1,2} + U_{2,1}U_{2,2} + U_{3,1}U_{3,2} \\ &= \left(U'_x - U''_z x_3 - U''_y x_2 - \theta''\phi\right)\left(-U'_y - \theta'\phi_{,2}\right) + \left(U'_z + \theta' x_2\right)\theta, \end{aligned} \tag{5b}$$

$$\begin{aligned} 2\eta_{13} &= U_{1,1}U_{1,3} + U_{2,1}U_{2,3} + U_{3,1}U_{3,3} \\ &= \left(U'_x - U''_z x_3 - U''_y x_2 - \theta''\phi\right)\left(-U'_z - \theta'\phi_{,3}\right) - \left(U'_y - \theta' x_3\right)\theta \end{aligned} \tag{5c}$$

and

$$e_{11}^* = U_{1,1}^* = \frac{1}{2}\left[-(\theta U'_z)' x_2 + \left(\theta U'_y\right)' x_3\right], \tag{6a}$$

$$2e_{12}^* = U_{1,2}^* + U_{2,1}^* = -\frac{1}{2}\left[\theta U'_z + \left(\theta^2 + U'^2_y\right)' x_2 + \left(U'_y U'_z\right)' x_3\right], \tag{6b}$$

$$2e_{13}^* = U_{1,3}^* + U_{3,1}^* = \frac{1}{2}\left[\theta U'_y - \left(U'_y U'_z\right)' x_2 - \left(\theta^2 + U'^2_z\right)' x_3\right], \tag{6c}$$

where e_{ij} and η_{ij} are the conventional linear and nonlinear strain due to U_i, respectively, and e_{ij}^* the linear strain due to U_i^*. Stress resultants in Fig. 1(b) are defined by

$$\begin{aligned} &F_1 = \int_A \tau_{11}\,\mathrm{d}A, \quad F_2 = \int_A \tau_{12}\,\mathrm{d}A, \quad F_3 = \int_A \tau_{13}\,\mathrm{d}A, \quad M_1 = \int_A (\tau_{13}x_2 - \tau_{12}x_3)\,\mathrm{d}A, \\ &M_2 = \int_A \tau_{11}x_3\,\mathrm{d}A, \quad M_3 = -\int_A \tau_{11}x_2\,\mathrm{d}A, \quad M_\phi = \int_A \tau_{11}\phi\,\mathrm{d}A, \quad M_p = \int_A \tau_{11}\left(x_2^2 + x_3^2\right)\mathrm{d}A, \end{aligned} \tag{7a–h}$$

where τ_{ij} is the second-Piola–Kirchhoff stress, F_1, F_2, and F_3, the axial force and shear forces, respectively, M_1 the total twisting moment with respect to the x_1-axis, M_2 and M_3 the bending moments with respect to x_2 and x_3 axes, respectively, M_ϕ the bimoment about the x_1 axis, and M_p the stress resultant as a Wagner effect.

Now, the total potential energy of a thin-walled beam element under consideration is expressed as

$$\Pi = \Pi_E + \Pi_G - \Pi_M - \Pi_{\text{ext}}, \tag{8}$$

where Π_E is the elastic strain energy, Π_G the potential energy due to combined effects of the initial stresses, body and surface forces, Π_M the kinetic energy, and Π_{ext} the potential energy due to the element nodal forces.

The detailed expressions for each term of the total potential energy are

$$\Pi_E = \frac{1}{2}\int_0^l \int_A \tau_{ij} e_{ij}\, \mathrm{d}A\, \mathrm{d}x_1, \tag{9a}$$

$$\Pi_G = \int_0^l \int_A \left[{}^0\tau_{ij}\left(\eta_{ij} + e^*_{ij}\right) - {}^0b_i U^*_i\right] \mathrm{d}A\, \mathrm{d}x_1 - \int_0^s {}^0T_i U^*_i\, \mathrm{d}s, \tag{9b}$$

$$\Pi_M = \frac{1}{2}\int_0^l \int_A \rho \dot{U}_i^2\, \mathrm{d}A\, \mathrm{d}x_1, \tag{9c}$$

$$\Pi_{\mathrm{ext}} = \frac{1}{2}\int_0^s \int_A T_i U_i\, \mathrm{d}s, \tag{9d}$$

where l and A are the element length and the area, respectively, ${}^0b_i$ and ${}^0T_i$ the body and surface forces, respectively, and ρ the density.

Substituting the displacement expansions in Eqs. (2) and (3) and the strain–displacement relations in Eqs. (4)–(6) into Eq. (9a–d), and integrating over the cross-section, Eq. (9a–d) can be expressed as

$$\begin{aligned}\Pi_E = \frac{1}{2}\int_0^l \Big[&EAU'^2_x + EI_2U''^2_z + EI_3U''^2_y + EI_\phi\theta''^2 + GJ\theta'^2 + 2EI_{23}U''_yU''_z \\ &+ 2EI_{\phi 2}U''_z\theta'' + 2EI_{\phi 3}U''_y\theta''\Big]\, \mathrm{d}x_1,\end{aligned} \tag{10a}$$

$$\begin{aligned}\Pi_G = \frac{1}{2}\int_0^l \Big[&{}^0F_1\left(U'^2_y + U'^2_z\right) + {}^0F_2U'_z\theta - {}^0F_3U'_y\theta + {}^0M_1\left(U''_yU'_z - U'_yU''_z\right) \\ &+ {}^0M_2\left(U''_y\theta - U'_y\theta'\right) + {}^0M_3\left(U''_z\theta - U'_z\theta'\right) + {}^0M_p\theta'^2\Big]\, \mathrm{d}x_1,\end{aligned} \tag{10b}$$

$$\begin{aligned}\Pi_M = \frac{1}{2}\rho\omega^2\int_0^l \Big[&A\left(U_x^2 + U_y^2 + U_z^2\right) + I_2U'^2_z + I_3U'^2_y + I_0\theta^2 + I_\phi\theta'^2 \\ &+ 2I_{23}U'_yU'_z + 2I_{\phi 2}U'_z\theta' + 2I_{\phi 3}U'_y\theta'\Big]\, \mathrm{d}x_1,\end{aligned} \tag{10c}$$

$$\Pi_{\mathrm{ext}} = \frac{1}{2}\mathbf{U}_e^{\mathrm{T}}\mathbf{F}_e, \tag{10d}$$

where E is the Young's modulus, G the shear modulus, J the torsional constant, and I_2, I_3, I_0, $I_{\phi 2}$, $I_{\phi 3}$ the sectional constants of which the detailed expressions may be referred to Kim and Kim [34], ω the circular frequency, and $\mathbf{U}_e$ and $\mathbf{F}_e$ the nodal displacement and nodal force vectors, respectively. And the linearly variable axial force ${}^0F_1$, the bending moment ${}^0M_2$ and ${}^0M_p$ can be expressed as

$${}^0F_1 = \xi x_1 + \zeta, \quad {}^0M_2 = {}^0F_3x_1, \quad {}^0M_p = (\xi x_1 + \zeta)\beta_1 + {}^0F_3x_1\beta_2, \tag{11a–c}$$

where the detailed definitions of β_1 and β_2 may be referred to Kim and Kim [34].

2.2. Equations of motion and force–deformation relations

By variation of Eq. (8) with respect to U_x, U_y, U_z, and θ, the equations of motion for thin-walled beam with non-symmetric cross-section subjected to linearly variable axial force are derived as

$$EAU''_x + \rho\omega^2AU_x = 0, \tag{12a}$$

$$\begin{aligned}&EI_3U''''_y + EI_{23}U''''_z + EI_{\phi 3}\theta'''' - \rho\omega^2\left(AU_y - I_3U''_y - I_{23}U''_z - I_{\phi 3}\theta''\right) - {}^0F'_1U'_y - {}^0F_1U''_y \\ &+ 2{}^0F_3\theta' + {}^0M_1U''''_z + {}^0M_2\theta'' = 0,\end{aligned} \tag{12b}$$

$$EI_2U_z'''' + EI_{23}U_y'''' + EI_{\phi 2}\theta'''' - \rho\omega^2\left(AU_z - I_2U''_z - I_{23}U''_y - I_{\phi 2}\theta''\right) - {}^0F'_1U'_z - {}^0F_1U''_z - {}^0M_1U'''_y + {}^0M_3\theta'' = 0, \tag{12c}$$

$$EI_\phi\theta'''' - GJ\theta'' + EI_{\phi 2}U_z'''' + EI_{\phi 3}U_y'''' - \rho\omega^2\left(I_0\theta - I_\phi\theta'' - I_{\phi 2}U''_z - I_{\phi 3}U''_y\right) + {}^0M_2U''_y + {}^0M_3U''_z - {}^0M_p\theta'' - \left({}^0F'_1\beta_1 + {}^0M'_2\beta_2\right)\theta' = 0. \tag{12d}$$

And force–deformation relations are

$$F_1 = EAU'_x, \tag{13a}$$

$$F_2 = -EI_3U'''_y - EI_{23}U'''_z - EI_{\phi 3}\theta''' - \rho\omega^2I_3U'_y - \rho\omega^2I_{23}U'_z - \rho\omega^2I_{\phi 3}\theta' + {}^0F_1U'_y - {}^0F_3\theta - {}^0M_1U''_z - {}^0M_2\theta', \tag{13b}$$

$$F_3 = -EI_2U'''_z - EI_{23}U'''_y - EI_{\phi 2}\theta''' - \rho\omega^2I_2U'_z - \rho\omega^2I_{23}U'_y - \rho\omega^2I_{\phi 2}\theta' + {}^0F_1U'_z + {}^0M_1U''_y - {}^0M_3\theta', \tag{13c}$$

$$M_1 = -EI_\phi\theta''' + GJ\theta' - EI_{\phi 2}U'''_z - EI_{\phi 3}U'''_y - \rho\omega^2I_\phi\theta' - \rho\omega^2I_{\phi 2}U'_z - \rho\omega^2I_{\phi 3}U'_y - 0.5{}^0M_2U'_y - 0.5{}^0M_3U'_z + {}^0M_p\theta', \tag{13d}$$

$$M_2 = -EI_2U''_z - EI_{23}U''_y - EI_{\phi 2}\theta'' + 0.5{}^0M_1U'_y - 0.5{}^0M_3\theta, \tag{13e}$$

$$M_3 = EI_3U''_y + EI_{23}U''_z + EI_{\phi 3}\theta'' + 0.5{}^0M_1U'_z + 0.5{}^0M_2\theta, \tag{13f}$$

$$M_\phi = -EI_\phi\theta'' - EI_{\phi 2}U''_z - EI_{\phi 3}U''_y. \tag{13g}$$

3. Evaluation of element stiffness matrices

In this chapter, the static and dynamic element stiffness matrices of thin-walled beam subjected to linearly variable axial force are evaluated. To this end, the axial displacement U_x may be supposed to be the linear function from Eq. 12(a) and the other three displacement state vectors consisting of 12 displacement parameters are considered as

$$d(x) = \left\langle U_y, U'_y, U''_y, U'''_y, U_z, U'_z, U''_z, U'''_z, \theta, \theta', \theta'', \theta''' \right\rangle^{\mathrm{T}}. \tag{14}$$

The solutions of three displacement parameters are taken as the following infinite power series:

$$U_y = \sum_{n=0}^{\infty} a_nx^n, \quad U_z = \sum_{n=0}^{\infty} b_nx^n, \quad \theta = \sum_{n=0}^{\infty} c_nx^n. \tag{15a–c}$$

Substituting Eqs. 15(a–c) into Eqs. 12(b–d) and shifting the index of power of x^n, we get the following equations:

$$\sum_{n=0}^{\infty}[EI_3(n+4)(n+3)(n+2)(n+1)a_{n+4} + EI_{23}(n+4)(n+3)(n+2)(n+1)b_{n+4} + EI_{\phi 3}(n+4)(n+3)(n+2)(n+1)c_{n+4} - \rho\omega^2\{Aa_n - I_3(n+2)(n+1)a_{n+2} - I_{23}(n+2)(n+1)b_{n+2} - I_{\phi 3}(n+2)(n+1)c_{n+2}\} - \xi(n+1)a_{n+1} - \xi(n+1)na_{n+1} - \zeta(n+2)(n+1)a_{n+2} + 2^0F_3(n+1)c_{n+1} + {}^0F_3(n+1)nc_{n+1} + {}^0M_1(n+3)(n+2)(n+1)b_{n+3}] = 0, \tag{16a}$$

$$\sum_{n=0}^{\infty}\big[EI_2(n+4)(n+3)(n+2)(n+1)b_{n+4}+EI_{23}(n+4)(n+3)(n+2)(n+1)a_{n+4}+EI_{\phi 2}(n+4)(n+3)(n+2)(n+1)c_{n+4}$$
$$-\rho\omega^2\{Ab_n-I_2(n+2)(n+1)b_{n+2}-I_{23}(n+2)(n+1)a_{n+2}-I_{\phi 2}(n+2)(n+1)c_{n+2}\}-\xi(n+1)b_{n+1}$$
$$-\xi(n+1)nb_{n+1}-\zeta(n+2)(n+1)b_{n+2}-{}^0M_1(n+3)(n+2)(n+1)a_{n+3}+{}^0M_3(n+2)(n+1)c_{n+2}\big]=0, \tag{16b}$$

$$\sum_{n=0}^{\infty}\big[EI_{\phi}(n+4)(n+3)(n+2)(n+1)c_{n+4}-GJ(n+2)(n+1)c_{n+2}+EI_{\phi 3}(n+4)(n+3)(n+2)(n+1)a_{n+4}$$
$$+EI_{\phi 2}(n+4)(n+3)(n+2)(n+1)b_{n+4}-\rho\omega^2\{I_0c_n-I_{\phi}(n+2)(n+1)c_{n+2}-I_{\phi 2}(n+2)(n+1)b_{n+2}$$
$$-I_{\phi 3}(n+2)(n+1)a_{n+2}\}+{}^0F_3(n+1)na_{n+1}-\xi\beta_1(n+1)nc_{n+1}-\zeta\beta_1(n+2)(n+1)c_{n+2}$$
$$-{}^0F_3\beta_2(n+1)nc_{n+1}-\xi\beta_1(n+1)c_{n+1}+{}^0M_3(n+2)(n+1)b_{n+2}-{}^0F_3\beta_2(n+1)c_{n+1}]=0, \tag{16c}$$

which can be compactly expressed in a matrix form

$$\mathbf{A}_n\{a_{n+4},b_{n+4},c_{n+4}\}^{\mathrm{T}}=\mathbf{B}_n\{a_n,a_{n+1},a_{n+2},a_{n+3},b_n,b_{n+1},b_{n+2},b_{n+3},c_n,c_{n+1},c_{n+2},c_{n+3}\}^{\mathrm{T}}. \tag{17}$$

The detailed components of $\mathbf{A}_n$ and $\mathbf{B}_n$ are

$$\mathbf{A}_n=\begin{bmatrix}\alpha_1 & \alpha_2 & \alpha_3\\ & \alpha_4 & \alpha_5\\ \text{symm.} & & \alpha_6\end{bmatrix}, \tag{18}$$

where

$$\alpha_1=EI_3(n+4)(n+3)(n+2)(n+1),\quad \alpha_2=EI_{23}(n+4)(n+3)(n+2)(n+1),$$
$$\alpha_3=EI_{\phi 3}(n+4)(n+3)(n+2)(n+1),\quad \alpha_4=EI_2(n+4)(n+3)(n+2)(n+1),$$
$$\alpha_5=EI_{\phi 2}(n+4)(n+3)(n+2)(n+1),\quad \alpha_6=EI_{\phi}(n+4)(n+3)(n+2)(n+1). \tag{19a–f}$$

And

$$\mathbf{B}_n=\begin{bmatrix}\gamma_1 & \gamma_2 & \gamma_3 & \cdot & \cdot & \cdot & \gamma_4 & \gamma_5 & \cdot & \gamma_6 & \gamma_7 & \cdot\\ \cdot & \cdot & \gamma_4 & -\gamma_5 & \gamma_1 & -\gamma_2 & \gamma_8 & \cdot & \cdot & \cdot & \gamma_9 & \cdot\\ \cdot & \gamma_{10} & \gamma_7 & \cdot & \cdot & \cdot & \gamma_9 & \cdot & \gamma_{11} & \gamma_{12} & \gamma_{13} & \cdot\end{bmatrix}, \tag{20}$$

where

$$\gamma_1=-\rho\omega^2A,\quad \gamma_2=-\xi(n+1)^2,\quad \gamma_3=\rho\omega^2I_3(n+2)(n+1)-\zeta(n+2)(n+1),\quad \gamma_4=\rho\omega^2I_{23}(n+2)(n+1),$$
$$\gamma_5={}^0M_1(n+3)(n+2)(n+1),\quad \gamma_6={}^0F_3(n+2)(n+1),\quad \gamma_7=\rho\omega^2I_{\phi 3}(n+2)(n+1),$$
$$\gamma_8=\rho\omega^2I_2(n+2)(n+1)-\zeta(n+2)(n+1),\quad \gamma_9=\rho\omega^2I_{\phi 2}(n+2)(n+1)+{}^0M_3(n+2)(n+1),\quad \gamma_{10}={}^0F_3(n+1)n,$$
$$\gamma_{11}=\rho\omega^2I_0,\quad \gamma_{12}=-\xi\beta_1(n+1)^2+{}^0F_3\beta_2(n+1)^2,\quad \gamma_{13}=\rho\omega^2I_{\phi}(n+2)(n+1)-\zeta\beta_1(n+2)(n+1). \tag{21a–m}$$

Also, Eq. (17) can be rewritten as

$$\{a_{n+4},b_{n+4},c_{n+4}\}^{\mathrm{T}}=Z_n\{a_n,a_{n+1},a_{n+2},a_{n+3},b_n,b_{n+1},b_{n+2},b_{n+3},c_n,c_{n+1},c_{n+2},c_{n+3}\}^{\mathrm{T}}, \tag{22}$$

where

$$\mathbf{Z}_n=\mathbf{A}_n^{-1}\mathbf{B}_n. \tag{23}$$

Thereafter, we put the initial integration constant vector

$$\mathbf{a}=\{a_0,a_1,a_2,a_3,b_0,b_1,b_2,b_3,c_0,c_1,c_2,c_3\}^{\mathrm{T}}. \tag{24}$$

Using Eq. (22), in case of $n=0$, 1 and $n=i$, we can obtain the following relations. For $n=0$,

$$\{a_4,b_4,c_4\}^{\mathrm{T}}=\mathbf{Z}_0\{a_0,a_1,a_2,a_3,b_0,b_1,b_2,b_3,c_0,c_1,c_2,c_3\}^{\mathrm{T}}=\mathbf{D}_2\mathbf{a}. \tag{25}$$

For $n = 1$,

$$\begin{aligned}\{a_5, b_5, c_5\}^{\mathrm{T}} &= \mathbf{Z}_1\{a_1, a_2, a_3, a_4, b_1, b_2, b_3, b_4, c_1, c_2, c_3, c_4\}^{\mathrm{T}} \\ &= \mathbf{Z}_1 \cdot \mathbf{N}_1\{a_0, a_1, a_2, a_3, b_0, b_1, b_2, b_3, c_0, c_1, c_2, c_3\}^{\mathrm{T}} \\ &= \mathbf{D}_3\mathbf{a}. \end{aligned} \tag{26}$$

For $n = i$ $(i \geqslant 2)$,

$$\begin{aligned}\{a_{i+4}, b_{i+4}, c_{i+4}\}^{\mathrm{T}} &= \mathbf{Z}_i\{a_i, a_{i+1}, a_{i+2}, a_{i+3}, b_i, b_{i+1}, b_{i+2}, b_{i+3}, c_i, c_{i+1}, c_{i+2}, c_{i+3}\}^{\mathrm{T}} \\ &= \mathbf{Z}_i \cdot \mathbf{N_i}\{a_0, a_1, a_2, a_3, b_0, b_1, b_2, b_3, c_0, c_1, c_2, c_3\}^{\mathrm{T}} \\ &= \mathbf{D}_{i+2}\mathbf{a}, \end{aligned} \tag{27}$$

where

$$\mathbf{N}_1 = \begin{bmatrix} & 1 & & \cdots\cdots\cdots\cdots & \\ D_2(1,1) & D_2(1,2) & D_2(1,3) & \cdots\cdots\cdots\cdots & D_2(1,12) \\ D_2(2,1) & D_2(2,2) & D_2(2,3) & \cdots\cdots\cdots\cdots & D_2(2,12) \\ D_2(3,1) & D_2(3,2) & D_2(3,3) & \cdots\cdots\cdots\cdots & D_2(3,12) \\ D_2(4,1) & D_2(4,2) & D_2(4,3) & \cdots\cdots\cdots\cdots & D_2(4,12) \\ D_2(5,1) & D_2(5,2) & D_2(5,3) & \cdots\cdots\cdots\cdots & D_2(5,12) \\ & & & & 1 \\ D_2(6,1) & D_2(6,2) & D_2(6,3) & & D_2(6,12) \end{bmatrix} \tag{28}$$

and

$$\mathbf{N_i} = \begin{bmatrix} D_i(1,1) & D_i(1,2) & D_i(1,3) & \cdots\cdots\cdots\cdots & D_i(1,12) \\ D_{i+1}(1,1) & D_{i+1}(1,2) & D_{i+1}(1,3) & \cdots\cdots\cdots\cdots & D_{i+1}(1,12) \\ D_i(2,1) & D_i(2,2) & D_i(2,3) & \cdots\cdots\cdots\cdots & D_i(2,12) \\ D_{i+1}(2,1) & D_{i+1}(2,2) & D_{i+1}(2,3) & \cdots\cdots\cdots\cdots & D_{i+1}(2,12) \\ D_i(3,1) & D_i(3,2) & D_i(3,3) & \cdots\cdots\cdots\cdots & D_i(3,12) \\ D_{i+1}(3,1) & D_{i+1}(3,2) & D_{i+1}(3,3) & \cdots\cdots\cdots\cdots & D_{i+1}(3,12) \\ D_i(4,1) & D_i(4,2) & D_i(4,3) & \cdots\cdots\cdots\cdots & D_i(4,12) \\ D_{i+1}(4,1) & D_{i+1}(4,2) & D_{i+1}(4,3) & \cdots\cdots\cdots\cdots & D_{i+1}(4,12) \\ D_i(5,1) & D_i(5,2) & D_i(5,3) & \cdots\cdots\cdots\cdots & D_i(5,12) \\ D_{i+1}(5,1) & D_{i+1}(5,2) & D_{i+1}(5,3) & \cdots\cdots\cdots\cdots & D_{i+1}(5,12) \\ D_i(6,1) & D_i(6,2) & D_i(6,3) & \cdots\cdots\cdots\cdots & D_i(6,12) \\ D_{i+1}(6,1) & D_{i+1}(6,2) & D_{i+1}(6,3) & \cdots\cdots\cdots\cdots & D_{i+1}(6,12) \end{bmatrix}, \tag{29}$$

where $D_i(j, k)$ denotes the component of D_i at jth row and kth column. By substituting the integration constants obtained by Eq. (27) into Eq. (15) and rearranging Eq. (14), the displacement state vector composed of 12 displacement parameters in Eq. (14) is expressed with respect to the initial integration constant vector **a** as follows:

$$\mathbf{d}(\mathbf{x}) = \mathbf{X}_n\mathbf{a}. \tag{30}$$

The initial integration constant vector **a** is represented with respect to 12 nodal displacement components. For this, the nodal displacement vectors at p and q which mean the two ends of the member ($x = 0$, l) is defined by

$$\mathbf{U}_e = \langle \mathbf{U}^p, \mathbf{U}^q \rangle^{\mathrm{T}}, \tag{31a}$$

$$\mathbf{U}^\alpha = \left\langle U_y^\alpha, U_z^\alpha, \omega_1^\alpha, \omega_2^\alpha, \omega_3^\alpha, f^\alpha \right\rangle^{\mathrm{T}}, \quad \alpha = p, q, \tag{31b}$$

where

$$\mathbf{U}^p = \left\langle U_y(0), U_z(0), \theta(0), -U_z'(0), U_y'(0), -\theta'(0) \right\rangle^{\mathrm{T}}, \tag{32a}$$

$$\mathbf{U}^q = \left\langle U_y(l), U_z(l), \theta(l), -U_z'(l), U_y'(l), -\theta'(l) \right\rangle^{\mathrm{T}}. \tag{32b}$$

Then, by substituting coordinates of the ends of member ($x = 0, l$) into Eq. (30) and accounting for Eq. (31), the nodal displacement vector $\mathbf{U}_e$ can be obtained as follows:

$$\mathbf{U}_e = \mathbf{H}\mathbf{a}. \tag{33}$$

Then, elimination of $\mathbf{a}$ from Eq. (30) using Eq. (33) yields the displacement state vector consisting of 12 displacement components:

$$\mathbf{d}(\mathbf{x}) = \mathbf{X}_n \mathbf{H}^{-1} \mathbf{U}_e, \tag{34}$$

where $\mathbf{X}_n\ \mathbf{H}^{-1}$denotes the interpolation matrix.

Next, we consider the nodal force vector at the two ends p and q defined by

$$\mathbf{F}_e = \langle \mathbf{F}^p, \mathbf{F}^q \rangle^{\mathrm{T}}, \tag{35}$$

where

$$\mathbf{F}^\alpha = \left\langle F_2^\alpha, F_3^\alpha, M_1^\alpha, M_2^\alpha, M_3^\alpha, M_\phi^\alpha \right\rangle^{\mathrm{T}}, \quad \alpha = p, q. \tag{36}$$

Also, the force–deformation relations in Eq. (13) can be expressed as a matrix form

$$\mathbf{f}(\mathbf{x}) = \mathbf{S}\mathbf{d}(\mathbf{x}) \tag{37}$$

in which

$$\mathbf{S} = \begin{bmatrix} \cdot & s_1 & \cdot & s_2 & \cdot & \cdot & s_3 & \cdot & \cdot & s_4 & \cdot & s_5 \\ \cdot & \cdot & -s_3 & \cdot & \cdot & s_6 & \cdot & s_7 & \cdot & s_8 & \cdot & s_9 \\ \cdot & s_{10} & \cdot & s_5 & \cdot & s_{11} & \cdot & s_9 & \cdot & s_{12} & \cdot & s_{13} \\ \cdot & -0.5s_3 & \cdot & \cdot & \cdot & \cdot & s_7 & \cdot & s_{14} & \cdot & s_9 & \cdot \\ \cdot & \cdot & -s_2 & \cdot & \cdot & -0.5s_3 & \cdot & \cdot & s_{15} & \cdot & -s_5 & \cdot \\ \cdot & \cdot & s_5 & \cdot & \cdot & \cdot & s_9 & \cdot & \cdot & \cdot & s_{13} & \cdot \end{bmatrix}, \tag{38}$$

where

$$\begin{aligned} &s_1 = (\xi x_1 + \zeta) - \rho\omega^2 I_3, \quad s_2 = -EI_3, \quad s_3 = -{}^0M_1, \quad s_4 = -{}^0M_2 - \rho\omega^2 I_{\phi 3}, \quad s_5 = -EI_{\phi 3}, \\ &s_6 = (\xi x_1 + \zeta) - \rho\omega^2 I_2, \quad s_7 = -EI_2, \quad s_8 = -{}^0M_3 - \rho\omega^2 I_{\phi 2}, \quad s_9 = -EI_{\phi 2}, \quad s_{10} = -0.5{}^0M_2 - \rho\omega^2 I_{\phi 3}, \\ &s_{11} = -0.5{}^0M_3 - \rho\omega^2 I_{\phi 2}, \quad s_{12} = GJ - \rho\omega^2 I_\phi + {}^0M_p, \quad s_{13} = -EI_\phi, \quad s_{14} = -0.5{}^0M_3, \\ &s_{15} = 0.5{}^0M_2. \end{aligned} \tag{39a–o}$$

Now substitution Eq. (34) into Eq. (37) leads to

$$\mathbf{f}(\mathbf{x}) = \mathbf{S}\mathbf{X}_n \mathbf{H}^{-1} \mathbf{U}_e. \tag{40}$$

And nodal forces at ends of the element are evaluated as

$$\mathbf{F}^p = -\mathbf{f}(0) = -\mathbf{S}\mathbf{X}_n(0)\mathbf{H}^{-1}\mathbf{U}_e, \tag{41a}$$

$$\mathbf{F}^q = \mathbf{f}(l) = \mathbf{S}\mathbf{X}_n(l)\mathbf{H}^{-1}\mathbf{U}_e. \tag{41b}$$

Consequently, the static stiffness matrix in the case that the natural frequency ω is zero and the dynamic stiffness matrix $\mathbf{K}$ of a thin-walled beam are calculated as follows:

$$\mathbf{F}_e = \mathbf{K}\mathbf{U}_e, \tag{42a}$$

where

$$\mathbf{K} = \begin{bmatrix} -\mathbf{S}\mathbf{X}_n(0)\mathbf{H}^{-1} \\ \mathbf{S}\mathbf{X}_n(l)\mathbf{H}^{-1} \end{bmatrix}. \tag{42b}$$

From the computational aspect, the buckling loads and natural frequencies of vibration of a member are those values of buckling load and frequency that cause the stiffness matrix to become singular, and one can find as many buckling loads and frequencies as needed from the same matrix. For a structure that is built of several cross-section members, the stiffness matrix is assembled as is usually done in finite element analysis using the direct stiffness method.

4. Finite element formulation

Fig. 2 shows the nodal displacement vector of a thin-walled beam element including the restrained warping effect. To accurately express the element deformation, pertinent shape functions are necessary. In this study, cubic Hermitian polynomials are adopted to interpolate displacement parameters that are defined at the centroid axis. This beam element has two nodes per one element and seven nodal degrees of freedom. As a result, assuming that axial displacement is linear, the element displacement parameters can be interpolated with respect to the nodal displacements as follows:

$$U_x = \alpha u^p + (1-\alpha)u^q, \quad \alpha = \frac{x_1}{l}, \tag{43a}$$

$$U_y = h_1 v^p + h_2 \omega_3^p + h_3 v^q + h_4 \omega_3^q, \tag{43b}$$

$$U_z = h_1 w^p - h_2 \omega_2^p + h_3 w^q - h_4 \omega_2^q, \tag{43c}$$

$$\theta = h_1 \omega_1^p - h_2 f^p + h_3 \omega_1^q - h_4 f^q, \tag{43d}$$

where

$$\begin{gathered} u^p = U_x(0), \quad v^p = U_y(0), \quad w^p = U_z(0), \\ \omega_1^p = \theta(0), \quad \omega_2^p = -U_z'(0), \quad \omega_3^p = U_y'(0), \quad f^p = -\theta'(0) \end{gathered} \tag{44a–g}$$

and h_i denotes cubic Hermitian polynomial as follows:

$$\begin{aligned} h_1 &= 2\alpha^3 - 3\alpha^2 + 1, \quad h_2 = \left(\alpha^3 - 2\alpha^2 + \alpha\right)l, \\ h_3 &= -2\alpha^3 + 3\alpha^2, \quad h_4 = \left(\alpha^3 - \alpha^2\right)l. \end{aligned} \tag{45a–d}$$

Substituting Eq. (43) into Eq. (10) and integrating along the element length, the equilibrium equations of a thin-walled beam are obtained in a matrix form. In this study, stiffness matrices and the mass matrix are evaluated using a Gauss numerical integration scheme.

5. Numerical examples

To demonstrate the accuracy and validity of this study, the flexural–torsional buckling and free vibration analysis of thin-walled beam with non-symmetric cross-section subjected to linearly variable axial force and

Fig. 2. Nodal displacement vector of a Hermitian beam element.

the lateral buckling analysis by the proposed method are performed and compared with the finite element solutions using the Hermitian beam elements and ABAQUS's shell elements. Particularly, the influence of constant and linearly variable axial force on the vibrational behavior of non-symmetric beam is investigated.

5.1. Buckling loads of beam subjected to constant axial force

Using the static element stiffness matrix by this study, the flexural–torsional buckling loads of cantilevered beam with non-symmetric cross-section, as shown in Fig. 3, subjected to constant axial force are evaluated. When the axial force acts at the centroid, numerical solutions by this study are evaluated and compared with those by the thin-walled beam elements and 600 nine-noded shell elements (S9R5) of ABAQUS in Table 1. Table 1 shows that the lowest five flexural–torsional buckling loads by this study, using only a single element, are in a good agreement with those by ABAQUS's shell elements. It should be noted that the present numerical solutions are accurate for the higher buckling modes as well as the lower ones because the displacement state vector in Eq. (34) satisfies the homogeneous form of the equilibrium equations. Still, a large number of Hermitian beam elements are required to achieve sufficient accuracy in the higher modes.

5.2. Free vibration analysis of beam subjected to constant axial force

In this example, the flexural–torsional free vibration analysis of cantilevered beam and clamped beam at both ends with non-symmetric cross-section subjected to constant axial force is performed. The same geometric and material data of beams as the one used in the previous example are adopted. Here, the buckling loads of cantilevered and clamped beams obtained from 20 Hermitian beam elements are 13.8 and 193.784 N, respectively. The values of 6.9 and 96.892 N are adopted as initial compressive and tensile forces for cantilevered and clamped beams, respectively, which are half of buckling loads of two beams.

The lowest ten coupled natural frequencies of cantilevered and clamped beams are presented in Tables 2 and 3, respectively. In general, it is not possible to derive the closed-form solution for the flexural–torsional vibration of cantilevered and clamped beams with non-symmetric cross-section. Hence, numerical solutions by this study are given and compared with the FE solutions obtained from various numbers of Hermitian beam elements. In particular, the results by 600 shell elements using S9R5 of ABAQUS are presented together for cantilevered and clamped beams without initial axial forces. From Tables 2 and 3, it can be found that this study yields accurate solutions by using only a single element, while at least 20 Hermitian beam elements are demanded for the reasonably good results in the higher vibrational modes. As shown in Tables 2 and 3, the

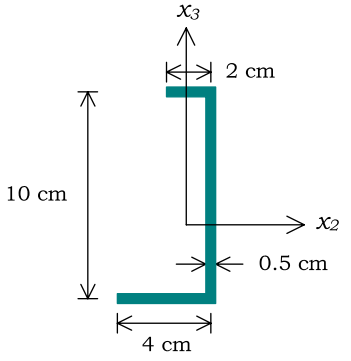

(a)

(b) $E = 30000\ \text{N/cm}^2$, $G = 11500\ \text{N/cm}^2$, $\rho = 0.00785\ \text{N/cm}^3$, $A = 8\ \text{cm}^2$, $J = 0.6667\ \text{cm}^4$, $l = 200\ \text{cm}$,
$I_2 = 113.54167\ \text{cm}^4$, $I_3 = 8.875\ \text{cm}^4$, $I_{23} = 11.875\ \text{cm}^4$, $I_\phi = 408.33333\ \text{cm}^6$, $I_{\phi 2} = 179.16667\ \text{cm}^5$,
$I_{\phi 3} = 39.16667\ \text{cm}^5$, $\beta_1 = 15.30208$, $\beta_2 = 0.71355$

Fig. 3. Cantilever beam with non-symmetric channel section: (a) non-symmetric channel section, (b) cantilever beam in the non-symmetric channel section.

Table 1
Flexural–torsional buckling loads for cantilevered beam (N)

Mode	Hermitian beam elements						ABAQUS 600-S9R5	This study ($n = 50$)
	4	6	8	10	20	40		
1	13.801	13.800	13.800	13.800	13.800	13.800	14.001	13.800
2	112.80	112.60	112.56	112.55	112.55	112.55	113.10	112.55
3	191.84	191.84	191.84	191.84	191.84	191.84	190.08	191.84
4	261.82	259.25	258.77	258.64	258.55	258.54	256.67	258.54
5	430.08	418.57	416.05	415.31	414.80	414.76	408.53	414.76

Table 2
Natural frequencies for cantilevered beam subjected to constant axial force [$(\text{rad/s})^2$] ($^0F_{1\text{cr}} = 13.8$ N)

Mode	Hermitian beam elements						ABAQUS 600-S9R5	This study ($n = 50$)
	4	6	8	10	20	40		
	(0.014)	(0.014)	(0.014)	(0.014)	(0.014)	(0.014)	—	(0.014)
1	0.027	0.027	0.027	0.027	0.027	0.027	0.028	0.027
	[0.039]	[0.039]	[0.039]	[0.039]	[0.039]	[0.039]	—	[0.039]
	(0.326)	(0.326)	(0.325)	(0.325)	(0.325)	(0.325)	—	(0.325)
2	0.337	0.337	0.336	0.336	0.336	0.336	0.331	0.336
	[0.348]	[0.347]	[0.347]	[0.347]	[0.347]	[0.347]	—	[0.347]
	(0.684)	(0.682)	(0.681)	(0.681)	(0.681)	(0.681)	—n	(0.681)
3	0.710	0.708	0.707	0.707	0.707	0.707	0.696	0.707
	[0.732]	[0.729]	[0.729]	[0.729]	[0.729]	[0.729]	—	[0.729]
	(1.006)	(1.005)	(1.004)	(1.004)	(1.004)	(1.004)	—	(1.004)
4	1.077	1.075	1.075	1.075	1.074	1.074	1.074	1.074
	[1.151]	[1.149]	[1.149]	[1.149]	[1.149]	[1.149]	—	[1.149]
	(4.799)	(4.765)	(4.758)	(4.756)	(4.754)	(4.754)	—	(4.754)
5	4.904	4.870	4.863	4.860	4.859	4.859	4.766	4.859
	[5.006]	[4.972]	[4.965]	[4.962]	[4.961]	[4.961]	—	[4.961]
	(7.114)	(7.042)	(7.027)	(7.023)	(7.020)	(7.019)	—	(7.019)
6	7.284	7.210	7.194	7.189	7.186	7.186	7.083	7.186
	[7.457]	[7.379]	[7.363]	[7.358]	[7.355]	[7.355]	—	[7.355]
	(18.39)	(18.09)	(18.00)	(17.98)	(17.96)	(17.96)	—	(17.96)
7	18.64	18.35	18.26	18.24	18.22	18.22	17.95	18.22
	[18.88]	[18.59]	[18.52]	[18.49]	[18.48]	[18.48]	—	[18.48]
	(20.14)	(20.05)	(20.01)	(20.00)	(19.99)	(19.99)	—	(19.99)
8	20.31	20.21	20.17	20.16	20.15	20.15	19.36	20.15
	[20.49]	[20.38]	[20.34]	[20.32]	[20.32]	[20.31]	—	[20.31]
	(24.63)	(24.33)	(24.21)	(24.18)	(24.15)	(24.15)	—	(24.15)
9	24.89	24.57	24.46	24.42	24.39	24.39	23.58	24.39
	[25.14]	[24.82]	[24.70]	[24.66]	[24.64]	[24.64]	—	[24.64]
	(56.80)	(47.96)	(47.21)	(46.95)	(46.76)	(46.75)	—	(46.75)
10	57.39	48.57	47.80	47.54	47.36	47.35	46.52	47.34
	[57.99]	[49.17]	[48.40]	[48.14]	[47.95]	[47.94]	—	[47.94]

Note: [ ] natural frequency with an initial compressive force 6.9 N.
( ) natural frequency with an initial tensile force 6.9 N.

Table 3
Natural frequencies for clamped beam subjected to constant axial force [(rad/s)^2] ($^0F_{1cr} = 193.784$ N)

Mode	Hermitian beam elements						ABAQUS 600-S9R5	This study ($n = 50$)
	4	6	8	10	20	40		
1	(0.443)	(0.440)	(0.440)	(0.440)	(0.440)	(0.440)	—	(0.440)
	0.915	0.911	0.911	0.910	0.910	0.910	0.914	0.910
	[1.377]	[1.369]	[1.368]	[1.367]	[1.367]	[1.367]	—	[1.367]
2	(2.684)	(2.667)	(2.663)	(2.662)	(2.661)	(2.661)	—	(2.661)
	3.144	3.123	3.118	3.116	3.115	3.115	3.046	3.115
	[3.602]	[3.575]	[3.569]	[3.566]	[3.565]	[3.565]	—	[3.565]
3	(4.135)	(4.069)	(4.056)	(4.053)	(4.050)	(4.050)	—	(4.050)
	5.912	5.827	5.811	5.806	5.803	5.803	5.780	5.803
	[7.681]	[7.567]	[7.545]	[7.538]	[7.534]	[7.533]	—	[7.533]
4	(15.55)	(15.10)	(14.97)	(14.93)	(14.90)	(14.90)	—	(14.90)
	18.02	17.74	17.69	17.68	17.66	17.66	17.24	17.66
	[19.79]	[19.49]	[19.44]	[19.42]	[19.41]	[19.41]	—	[19.41]
5	(16.25)	(15.98)	(15.94)	(15.92)	(15.91)	(15.91)	—	(15.91)
	9.39	18.82	18.67	18.63	18.60	18.60	18.31	18.60
	[20.93]	[20.84]	[20.82]	[20.81]	[20.81]	[20.81]	—	[20.81]
6	(20.11)	(20.07)	(20.06)	(20.05)	(20.05)	(20.05)	—	(20.05)
	20.71	20.63	20.61	20.61	20.61	20.61	19.20	20.61
	[23.60]	[22.88]	[22.71]	[22.67]	[22.63]	[22.63]	—	[22.63]
7	(50.57)	(39.48)	(38.68)	(38.44)	(38.27)	(38.26)	—	(38.26)
	57.76	46.16	45.29	45.02	44.84	44.83	43.99	44.83
	[64.95]	[52.84]	[51.88]	[51.60]	[51.41]	[51.40]	—	[51.40]
8	(57.73)	(56.00)	(55.47)	(55.31)	(55.21)	(55.21)	—	(55.20)
	61.69	59.82	59.28	59.12	59.02	59.01	56.81	59.01
	[65.66]	[63.64]	[63.08]	[62.93]	[62.82]	[62.81]	—	[62.81]
9	(129.9)	(84.56)	(83.01)	(81.92)	(81.15)	(81.10)	—	(81.10)
	141.7	95.08	93.21	92.07	91.27	91.22	87.77	91.21
	[153.5]	[105.6]	[103.4]	[102.2]	[101.4]	[101.3]	—	[101.3]
10	(152.9)	(148.9)	(145.6)	(144.5)	(143.7)	(143.6)	—	(143.6)
	154.6	152.2	151.2	150.6	150.1	150.1	127.6	150.1
	[156.4]	[154.1]	[153.6]	[153.4]	[153.3]	[153.3]	—	[153.3]

Note: [ ] natural frequency with an initial compressive force 96.892 N.
( ) natural frequency with an initial tensile force 96.892 N.

present solutions are in good agreement with those of ABAQUS' shell elements. Also, the influence of initial compressive and tensile forces on the coupled natural frequencies is predominant in the first few modes. Figs. 4 and 5, respectively, show the relative difference of the first two natural frequencies for beams subjected to initial compressive and tensile forces versus various lengths of beam. Here, ω_C and ω_T denote the frequency including the initial compressive force and tensile force, respectively. It can be observed from Figs. 4 and 5 that the effect of initial axial forces on the fundamental frequency of clamped beam is the same as the 50% ratio of these forces to buckling loads. However, those effects for cantilevered beam are a little smaller than those of clamped beam.

5.3. Buckling and free vibration analysis of beam subjected to linearly variable axial force

This example concerns the cantilevered beam subjected to linearly variable axial compressive force, which is $^0F_1$ at free end and 2^0F_1 at fixed end. In this case, due to the variable axial force, the buckling loads and the

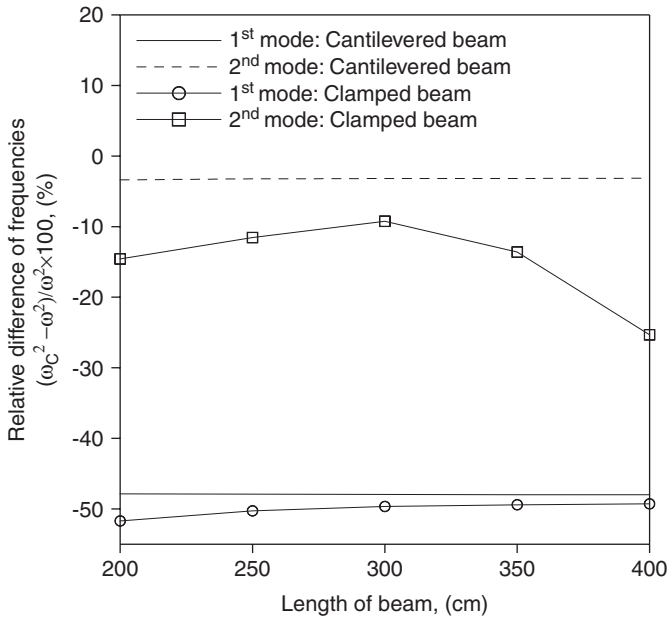

Fig. 4. Relative difference of natural frequencies versus length of beam due to initial compressive force.

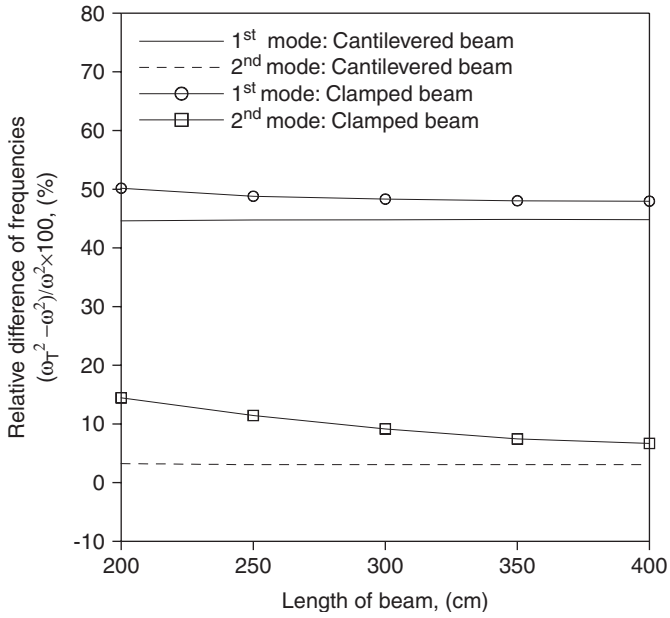

Fig. 5. Relative difference of natural frequencies versus length of beam due to initial tensile force.

natural frequencies cannot be determined by the approach proposed by Kim et al. [27]. In Table 4, the flexural–torsional buckling loads by this study are presented and compared with the FE solutions obtained from various numbers of Hermitian beam elements. As shown in Table 4, in the current study only a single element gives the buckling loads of thin-walled beam with non-symmetric cross-section subjected to linearly variable axial force.

Table 4
Flexural–torsional buckling loads for cantilevered beam subjected to linearly variable axial force (N)

Mode	Hermitian beam elements					This study ($n = 50$)
	2	6	10	20	40	
1	10.607	10.601	10.601	10.601	10.601	10.601
2	78.016	76.920	76.886	76.881	76.880	76.880
3	146.83	146.74	146.74	146.74	146.74	146.74
4	210.26	174.11	173.63	173.56	173.56	173.56
5	341.27	281.17	278.76	278.35	278.32	278.32

Table 5
Natural frequencies for cantilevered beam subjected to linearly variable axial force [(rad/s)^2] ($^0F_{1cr} = 10.601$ N)

Mode	Hermitian beam elements						This study ($n = 50$)
	4	6	8	10	20	40	
1	0.014 (0.000)	0.014 (0.000)	0.014 (0.000)	0.014 (0.000)	0.014 (0.000)	0.014 (0.000)	0.014 (0.000)
2	0.325 (0.313)	0.325 (0.312)	0.324 (0.312)	0.324 (0.312)	0.324 (0.312)	0.324 (0.312)	0.324 (0.312)
3	0.683 (0.650)	0.681 (0.648)	0.681 (0.648)	0.681 (0.648)	0.681 (0.648)	0.681 (0.648)	0.681 (0.648)
4	1.007 (0.944)	1.006 (0.942)	1.005 (0.942)	1.005 (0.942)	1.005 (0.942)	1.005 (0.942)	1.005 (0.942)
5	4.789 (4.672)	4.757 (4.641)	4.750 (4.635)	4.748 (4.633)	4.748 (4.633)	4.748 (4.634)	4.748 (4.634)
6	7.105 (6.930)	7.034 (6.863)	7.020 (6.849)	7.016 (6.845)	7.014 (6.844)	7.014 (6.844)	7.014 (6.845)
7	18.37 (18.08)	18.07 (17.77)	17.98 (17.69)	17.96 (17.66)	17.94 (17.65)	17.94 (17.65)	17.94 (17.65)
8	20.13 (19.96)	20.04 (19.88)	20.00 (19.84)	19.99 (19.83)	19.99 (19.83)	19.99 (19.83)	19.99 (19.83)
9	24.61 (24.34)	24.31 (24.05)	24.19 (23.94)	24.16 (23.91)	24.14 (23.89)	24.14 (23.89)	24.14 (23.89)
10	56.75 (56.10)	47.91 (47.25)	47.15 (46.50)	46.90 (46.25)	46.71 (46.07)	46.70 (46.06)	46.70 (46.06)

Note: ( ) natural frequency with an initial compressive force $^0F_{1cr}$.

Next, the coupled natural frequencies of beam subjected to linearly variable axial force, which have half of buckling load and buckling load are presented in Table 5. The excellent agreement between results from this study using a single element and those from 20 beam elements is evident. Additionally, the relative difference of the first two natural frequencies for cantilevered beam subjected to linearly variable compressive force, which is half the value of fundamental buckling load, is depicted in Fig. 6 with respect to the length of beam. From Fig. 6, it is interesting to note that the influence of linearly variable axial force on frequencies is the same as that of beam with constant axial force.

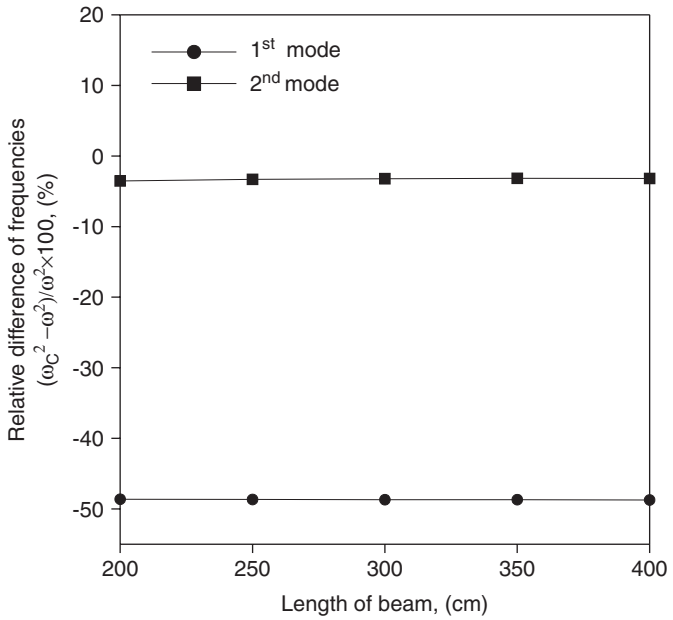

Fig. 6. Relative difference of natural frequencies of cantilevered beam versus length of beam due to linearly variable compressive force.

Table 6
Lateral buckling loads subjected to vertical loads (N)

Hermitian beam elements					ABAQUS 1800-S8R5	This study ($n = 50$)
2	6	10	20	40		
−4.4315	−4.2595	−4.2569	−4.2564	−4.2564	−4.1086	−4.2564
6.1114	5.8132	5.7987	5.7957	5.7955	5.8933	5.7954

5.4. Lateral buckling analysis

The purpose of our final example is to evaluate the lateral buckling loads for the thin-walled beam with non-symmetric cross-section. The beam with cross-section, as shown in Fig. 3, subjected to the lateral tip load at the centroid of the free end is considered. In Table 6, the results of this study are given and compared with the results of Hermitian beam elements and ABAQUS solutions using 1600 eight-noded shell elements (S8R5), which is modeled by Kim et al. [35]. It can be observed from Table 6, the solutions in this study are greatly in agreement with the solutions by ABAQUS's shell elements. Therefore, it is judged that the present formulation and method developed can predict lateral buckling loads of non-symmetric thin-walled beam.

6. Conclusion

For the flexural–torsional buckling and free vibration analysis of thin-walled beam with non-symmetric cross-section subjected to linearly variable axial force, the static and dynamic stiffness matrices are newly presented based on the power series method. In addition, the static stiffness matrix for the lateral buckling analysis of non-symmetric beam is presented for the first time.

Through the numerical examples, it is demonstrated that results from this study using only a single element have shown to be in excellent agreement with the solutions using Hermitian beam element and ABAQUS's

shell elements. It is believed that the proposed beam element eliminates discretization errors and is capable of predicting an infinite number of buckling loads and natural frequencies of beams by means of a finite number of coordinates. Also, the influence of constant and linearly variable axial forces on vibration behavior is investigated.

Acknowledgments

This work is a part of a research project supported by Korea Ministry of Construction & Transportation through Korea Bridge Design & Engineering Research Center at Seoul National University. The authors wish to express their gratitude for the financial support.

References

[1] V.Z. Vlasov, 1961, Thin-walled elastic beams, second ed., *Israel Program for Scientific Transactions*, Jerusalem.
[2] S.P. Timoshenko, J.M. Gere, *Theory of Elastic Stability*, second ed., McGraw-Hill, New York, 1961.
[3] R.W. Barsoum, R.H. Gallagher, Finite element analysis of torsional and torsional–flexural stability problems, *International Journal for Numerical Methods in Engineering* 2 (1970) 335–352.
[4] W.F. Chen, T. Atsuta, *Theory of Beam—Columns, Space Behavior and Design*, Vol. 2, McGraw-Hill, New York, 1977.
[5] M.M. Attard, Lateral buckling analysis of beams by the FEM, *Computers & Structures* 23 (1985) 217–231.
[6] S. Kitipornchai, N.S. Trahair, Buckling properties of monosymmetric I—beams, *Journal of Structural Division, ASCE* 106 (1980) 941–958.
[7] T.M. Roberts, C.A. Burt, Instability of monosymmetric I—beams and cantilevers, *International Journal of Mechanical Sciences* 27 (1985) 313–324.
[8] C.T. Sun, S.N. Huang, Transverse impact problems by higher order beam finite element, *Computers & Structures* 5 (1975) 297–303.
[9] B.A. Coulter, R.E. Miller, Vibration and buckling of beam—columns subjected to non-uniform axial loads, *International Journal for Numerical Methods in Engineering* 23 (1986) 1739–1755.
[10] N.G. Park, S.K. Lee, H.K. Kim, K.S. Choi, Vibration of initially stressed beam with discretely spaced multiple elastic supports, *KSME International Journal* 18 (2004) 733–741.
[11] A. Andrade, D. Camotim, Lateral–torsional buckling of singly symmetric tapered beams: theory and applications, *Journal of Engineering Mechanics* 131 (2006) 586–597.
[12] N. Silvestre, D. Camotim, Distortional buckling formulae for cold-formed steel C and Z-section members part I—derivation, *Thin-Walled Structures* 42 (2004) 1567–1597.
[13] C. Yu, B.W. Schafer, Distortional buckling tests on cold-formed steel beams, *Journal of Structural Engineering* 132 (2006) 515–528.
[14] C. Yu, B.W. Schafer, Local buckling tests on cold-formed steel beams, *Journal of Structural Engineering* 129 (2003) 1596–1606.
[15] P.O. Friberg, Coupled vibrations of beams—an exact dynamic element stiffness matrix, *International Journal for Numerical Methods in Engineering* 19 (1983) 479–493.
[16] J.R. Banerjee, Free vibration of axially loaded composite Timoshenko beams using the dynamic stiffness matrix method, *Computers & Structures* 69 (1998) 197–208.
[17] J.R. Banerjee, Dynamic stiffness formulation for structural elements: a general approach, *Computers & Structures* 63 (1997) 101–103.
[18] J.R. Banerjee, Coupled bending–torsional dynamic stiffness matrix for beam elements, *International Journal for Numerical Methods in Engineering* 28 (1989) 1283–1298.
[19] J.R. Banerjee, F.W. Williams, Exact dynamic stiffness matrix for composite Timoshenko beams with applications, *Journal of Sound and Vibration* 194 (1996) 573–585.
[20] J.R. Banerjee, F.W. Williams, Coupled bending–torsional dynamic stiffness matrix of an axially loaded Timoshenko beam element, *International Journal of Solids and Structures* 31 (1994) 749–762.
[21] J.R. Banerjee, F.W. Williams, Coupled bending–torsional dynamic stiffness matrix for Timoshenko beam elements, *Computers & Structures* 42 (1992) 301–310.
[22] J.R. Banerjee, S.A. Fisher, Coupled bending–torsional dynamic stiffness matrix for axially loaded beam elements, *International Journal for Numerical Methods in Engineering* 33 (1992) 739–751.
[23] A.Y.T. Leung, S.P. Zeng, Analytical formulation of dynamic stiffness, *Journal of Sound and Vibration* 177 (1994) 555–564.
[24] D.M. Lee, M.J. Choi, T.Y. Oh, Transfer matrix modeling for the 3-dimensional vibration analysis of piping system containing fluid flow, *KSME International Journal* 10 (1996) 180–189.
[25] A.Y.T. Leung, Dynamic stiffness for lateral buckling, *Computers & Structures* 42 (1992) 321–325.
[26] W.R. Spillers, S. Rashidi, Member stiffness for three-dimensional beam-columns, *Journal of Structural Engineering* 123 (1997) 971–972.
[27] M.Y. Kim, N.I. Kim, H.T. Yun, Exact dynamic and static stiffness matrices of shear deformable thin-walled beam-columns, *Journal of Sound and Vibration* 267 (2003) 29–55.
[28] J.H. Argyris, P.C. Dunne, D.W. Scharpf, On large displacement-small strain analysis of structures of rotational degrees of freedom, *Computer Methods in Applied Mechanics and Engineering* 14 (1978) 401–451.

[29] J.H. Argyris, O. Hilpert, G.A. Malejannakis, D.W. Scharpf, On the geometrical stiffness of a beam in space—a consistent V.W. approach, *Computer Methods in Applied Mechanics and Engineering* 20 (1979) 105–131.
[30] H. Ziegler, *Principles of Structural Stability*, McGraw-Hill, New York, 1973.
[31] H. Chen, G.E. Blandford, Thin-walled space frames. I: large deformation analysis theory, *Journal of Structural Engineering* 117 (1991) 2499–2520.
[32] L.H. Teh, M.J. Clarke, New definition of conservative internal moments in space frames, *Journal of Engineering Mechanics* 123 (1997) 97–106.
[33] L.H. Teh, M.J. Clarke, Symmetry of tangent stiffness matrices of 3D elastic frame, *Journal of Engineering Mechanics* 125 (1999) 248–251.
[34] S.B. Kim, M.Y. Kim, Improved formulation for spatial stability and free vibration of thin-walled tapered beams and space frames, *Engineering Structures* 22 (2000) 446–458.
[35] M.Y. Kim, S.P. Chang, S.B. Kim, Spatial stability analysis of thin-walled space frames, *International Journal for Numerical Methods in Engineering* 39 (1996) 499–525.